

Enhanced magnetization in proton irradiated $\text{Mn}_3\text{Si}_2\text{Te}_6$ van der Waals crystals

Cite as: Appl. Phys. Lett. **116**, 172404 (2020); <https://doi.org/10.1063/5.0002168>

Submitted: 22 January 2020 . Accepted: 09 April 2020 . Published Online: 28 April 2020

L. M. Martinez, H. Iturriaga , R. Olmos , L. Shao , Y. Liu , Thuc T. Mai, C. Petrovic , Angela R. Hight Walker, and S. R. Singamaneni



View Online



Export Citation



CrossMark

ARTICLES YOU MAY BE INTERESTED IN

[Discovery of multiferroics with tunable magnetism in two-dimensional lead oxide](#)

Applied Physics Letters **116**, 172105 (2020); <https://doi.org/10.1063/1.5144842>

[Tunable magnetic properties in van der Waals crystals \$\(\text{Fe}_{1-x}\text{Co}_x\)_5\text{GeTe}_2\$](#)

Applied Physics Letters **116**, 202402 (2020); <https://doi.org/10.1063/5.0006337>

[Generation, electric detection, and orbital-angular momentum tunneling of twisted magnons](#)

Applied Physics Letters **116**, 172403 (2020); <https://doi.org/10.1063/5.0005764>

Lock-in Amplifiers
up to 600 MHz



Watch



Enhanced magnetization in proton irradiated $\text{Mn}_3\text{Si}_2\text{Te}_6$ van der Waals crystals

Cite as: Appl. Phys. Lett. **116**, 172404 (2020); doi: 10.1063/5.0002168

Submitted: 22 January 2020 · Accepted: 9 April 2020 ·

Published Online: 28 April 2020



View Online



Export Citation



CrossMark

L. M. Martinez,¹ H. Iturriaga,¹  R. Olmos,¹  L. Shao,²  Y. Liu,³  Thuc T. Mai,⁴ C. Petrovic,³ 
Angela R. Hight Walker,⁴ and S. R. Singamaneni^{1,a)}

AFFILIATIONS

¹Department of Physics, The University of Texas at El Paso, El Paso, Texas 79968, USA

²Department of Nuclear Engineering, Texas A&M University, College Station, Texas 77845, USA

³Condensed Matter Physics and Materials Science Department, Brookhaven National Laboratory, Upton, New York 11973, USA

⁴Nanoscale Device Characterization Division, Physical Measurement Laboratory, National Institute of Standards and Technology, Gaithersburg, Maryland 20899, USA

a) Author to whom correspondence should be addressed: srao@utep.edu

ABSTRACT

van der Waals (vdW) engineering of magnetism is a topic of increasing research interest in the community at present. We study the magnetic properties of quasi-two-dimensional layered vdW $\text{Mn}_3\text{Si}_2\text{Te}_6$ (MST) crystals upon proton irradiation as a function of fluences of 1×10^{15} , 5×10^{15} , 1×10^{16} , and 1×10^{18} H^+/cm^2 . We find that the magnetization is significantly enhanced by 53 % and 37 % in the ferrimagnetic phase (at 50 K) when the MST crystal was irradiated with the proton fluence of 5×10^{15} , both in *ab* and *c* planes, respectively. The ferrimagnetic ordering temperature and magnetic anisotropy are retained even after proton irradiation. From the fluence dependence of magnetization, electron paramagnetic resonance spectral parameters (*g*-value and signal width), and Raman data, we show that the magnetic exchange interactions (Mn–Te–Mn) are significantly modified at this fluence. This work shows that it is possible to employ proton irradiation in tuning the magnetic properties of vdW crystals and provide many opportunities to design desired magnetic phases.

Published under license by AIP Publishing. <https://doi.org/10.1063/5.0002168>

The manipulation of the physical properties of materials through irradiation or photo-excitation has been of particular interest for electronic device functionality in space^{1–3} and the fundamental understanding of the interaction between light and matter.^{4–7} In particular, proton irradiation is known as one of the main sources that hinders the electrical properties of electronics in spacecraft undergoing tasks near Earth's orbit.^{8,9} However, proton irradiation has the potential to positively impact the magnetic characteristics of materials.¹⁰ Studies have shown that irradiation with protons induces ferromagnetic ordering in some materials such as MoS_2 and graphite, materials that are normally non-magnetic.^{11–19} For example, MoS_2 has been a popular van der Waals (vdW) material to study due to its similarities to graphene, while maintaining the benefits of a large direct bandgap (1.8 eV), good electrical properties, and catalytic activity.^{20–24} Using proton irradiation, Mathew *et al.*¹⁶ introduced magnetic ordering in MoS_2 , which resulted in a change from diamagnetic to ferrimagnetic behavior above room temperature, attributed to vacancies and edge states produced by proton irradiation. Another study by Wang *et al.* shows a change in the bandgap of MoS_2 due to defects that trap

excitons after irradiation.¹ In the case of graphite, exposure to irradiation¹¹ yielded ferromagnetic ordering. vdW materials have recently raised interest due to the ability to exfoliate the bulk crystals down to a few- or mono-layers and still retain and/or improve their pristine magnetic properties.^{25–28} Even though many studies have emerged on these vdW materials, there are various materials, in that family, which have remained less explored in bulk or few-layer form. $\text{Mn}_3\text{Si}_2\text{Te}_6$ (MST), similar to $\text{Cr}_2\text{Si}_2\text{Te}_6$ (CST), which is another vdW magnet, is a part of the vdW family of layered materials that has only recently received some renewed interest.^{29,30} May and co-authors³⁰ determined the trigonal crystal structure, containing MnTe_6 octahedra that share edges within the *ab*-plane (Mn1 site). In MST, one-third of the Mn atoms link the layers together by filling the octahedral holes (Mn2 site) within the vdW gap, and these two sites are antiferromagnetically aligned. Later on, Liu and Petrovic performed a study²⁹ on the critical behavior of MST and confirmed a ferrimagnetic temperature (T_C) of ≈ 74 K.

To date, various strategies such as electrostatic gating, pressure, and iso-valent alloying have been employed to control magnetism in

2D layered magnets. Using proton irradiation, we hope to modify the magnetic properties of MST as a function of proton fluence, which was unreported earlier. However, proton irradiation is uncommon on Earth, but represents a majority of cosmic radiation incident to the Earth's atmosphere. Studying the effects of proton irradiation on vdWs materials can give clues as to their general behavior when irradiated in space environments as exemplified in recent reviews^{10,31} and reports.³²

In this study, we irradiated MST with protons at an energy of 2 MeV at the different proton fluences of 1×10^{15} , 5×10^{15} , 1×10^{16} , and 1×10^{18} H^+/cm^2 . A non-linear change in the magnetization (measured from hysteresis loops) was observed as a function of proton fluence. We noticed no dramatic change in T_C upon proton irradiation. Electron paramagnetic resonance (EPR) measurements show two signals corresponding to Mn^{2+} paramagnetic centers, assigned to Mn1 and Mn2 sites. No additional signals were observed, indicating the absence of magnetic defects that may have been formed after irradiation. EPR data coupled with the Raman data suggest that the proton irradiation modifies the exchange interactions in MST and may have played a key role in the modification of magnetization.

MST single crystals (mm in lateral dimensions, <0.5 mm in thickness) were prepared as reported previously by some of us (Y.L. and C.P.).²⁹ A Quantum Design Versalab System with a temperature range of 50 K–400 K and a magnetic field range of ± 3 T was used for this study. The magnetic field was applied in the ab plane, as well as in the c plane. The EPR spectra were recorded on a Bruker EMX Plus X-band (≈ 9.43 GHz) spectrometer, equipped with a high sensitivity probe head. A Cold-EdgeTM ER 4112HV In-Cavity Cryo-Free VT system connected with an Oxford temperature measurement was used in combination with the EPR spectrometer. All the samples were carefully handled with nonmagnetic capsules and Teflon tapes to avoid contamination. The 2 MeV proton irradiation was performed by using a 1.7 MV Tandatron accelerator. This energy was chosen to avoid unwanted damage in the crystal. The projected range was $30 \mu\text{m}$, and the damage profile has a relative flat distribution from the surface up to $30 \mu\text{m}$ (supplementary material, Fig. S1). The beam current was 100 nA. The beam spot size was $6 \text{ mm} \times 6 \text{ mm}$, and the beam was rastered over an area of $1.2 \text{ cm} \times 1.2 \text{ cm}$ to guarantee lateral beam uniformity. The weak beam current and the beam rastering reduce the beam heating ($<50^\circ\text{C}$) during irradiation. The beam was filtered using multiple magnet bending devices to remove carbon contamination.^{33,34} The vacuum during the irradiation was 6×10^{-8} Torr or better. The application of liquid nitrogen trapping during irradiation was performed to improve vacuum. Proton irradiation was carried out on separate crystals for each fluence. Raman spectra were collected in parallel geometry using a Renishaw Raman spectrometer using 532 nm laser wavelength excitation with 15 s count and a $50\times$ optical microscope objective.

To study the variation of magnetization as a function of proton fluence, the isothermal (50 K) magnetization measurements were performed as a function of proton fluence, both in the ab and c planes in the ferrimagnetic phase, and the data are plotted in Figs. 1(a) and 1(b). To compare, isothermal magnetization variation for the pristine crystal (shown with the curve in black) in both the directions is also included. As shown in Fig. 1(a) for the ab plane, square-shaped M–H loops are observed at all the fluences, associated with a negligible coercive field, consistent with previous reports.^{29,30} Most interestingly, the

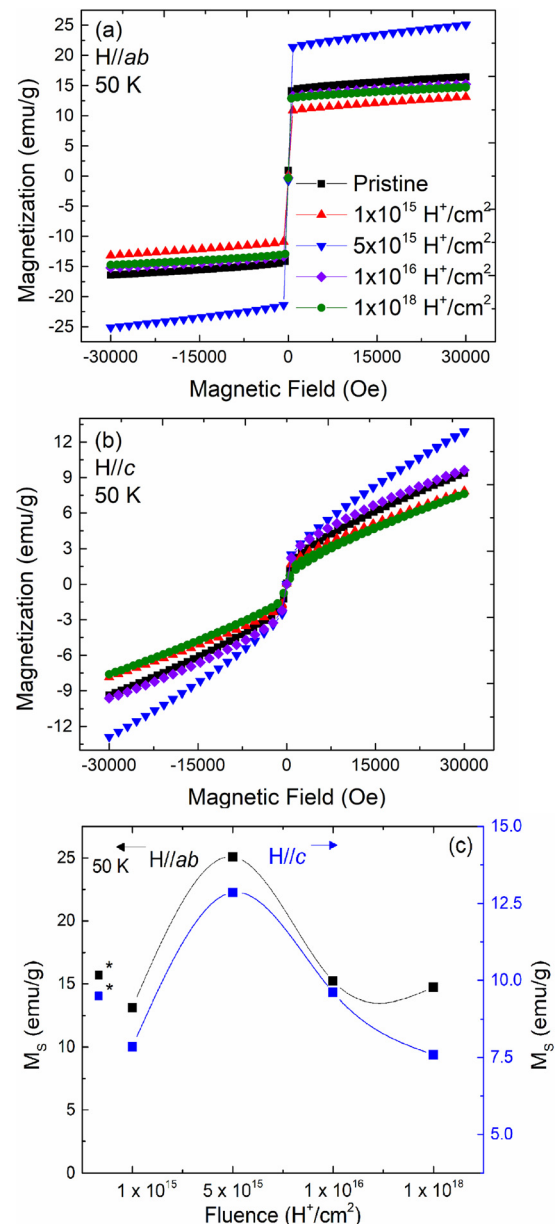


FIG. 1. Isothermal magnetization measured in the ab plane (a) and in the c plane (b) performed in the ferrimagnetic phase at 50 K. The fluence dependent magnetization is shown; the left y-axis represents the magnetization collected in the ab plane, and the right y-axis shows the magnetization collected in the c plane (c).

ab plane magnetization observed at 50 K is enhanced by about 53 % when the MST crystal was irradiated with the proton fluence of 5×10^{15} H^+/cm^2 , in comparison to that of the pristine crystal. A similar trend is observed even when the magnetization was measured in the c plane as depicted in Fig. 1(b) as the magnetization in the c plane is known^{29,30} to have small ferromagnetic contribution. Figures 1(a) and 1(b) show that the strong magnetic anisotropy is retained even after proton irradiation. The magnetization in the ab plane is higher

than that in the c plane as ordered moments lie primarily within the ab plane in agreement with the previous reports on MST.^{29,30} No remanent moment for either orientation confirms that the crystal retains its high quality even after proton irradiation.

The trends in the magnetization as a function of proton fluence are captured in Fig. 1(c), for both ab and c plane magnetization. As it can be immediately evidenced, the highest magnetization value was observed for the isothermal magnetization measurement irradiated with a proton fluence of $5 \times 10^{15} \text{ H}^+/\text{cm}^2$, with an increase of 53 % with respect to its pristine value. The magnetization decreased when MST was irradiated with fluences of 1×10^{16} and $1 \times 10^{18} \text{ H}^+/\text{cm}^2$. Here, the magnetization value is taken for all the samples measured at 50 K and 3 T from Figs. 1(a) and 1(b).

To study T_C as a function of proton fluence, the temperature dependent magnetization measurements were performed, in both the ab and c planes, plotted in the supplementary material, Figs. S2(a) and S2(b). The dM/dT (Fig. 2) curves show no significant change in T_C upon proton irradiation. In the pristine MST, T_C was found at $\approx 74 \text{ K}$,

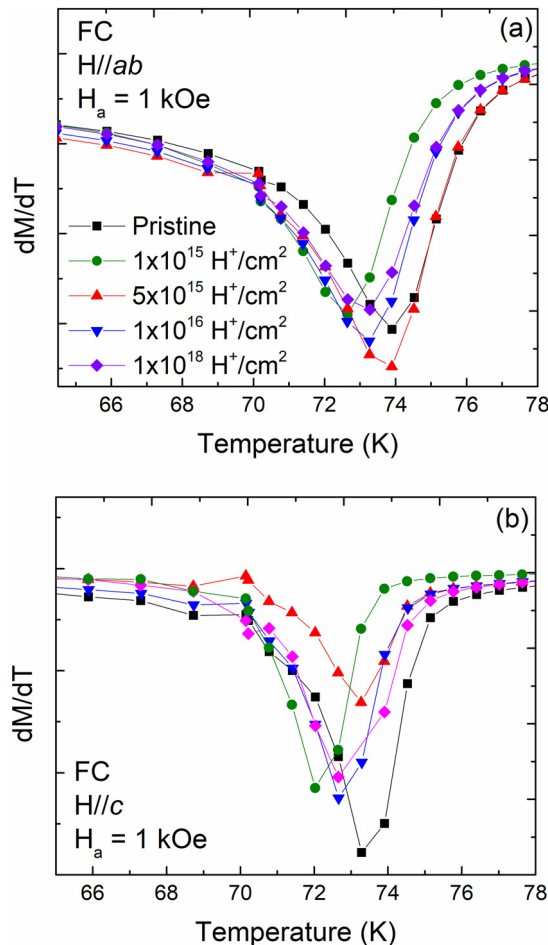


FIG. 2. dM/dT curves obtained from magnetization vs temperature curves for pristine and all the proton fluence applied to MST. The curves are presented in both the out-of-plane (a) and the in-plane direction (b) from the field-cooled (FC) curves measured with an applied (and cooling) field of 1 kOe.

in good agreement with previous reports.^{29,30} The most noticeable change in T_C was observed after a proton fluence of $1 \times 10^{18} \text{ H}^+/\text{cm}^2$ with a small decrease of 1.4 K (supplementary material, Table S1). The $1/\chi$ vs T plots (supplementary material, Fig. S3) were fitted using the Curie-Weiss law, $\chi = C/(T - \theta_W)$, in order to extract the Weiss temperature (θ_W). The fits were done with the temperature range of 200 K–400 K, and the resulting θ_W values are displayed in the supplementary material, Table S1. The extracted T_C was found to be negative, indicating antiferromagnetic correlations³⁰ and almost three times greater than the T_C estimated from dM/dT curves. The effective moment is consistent with the presence of Mn^{2+} ions, also supported by EPR measurements (see below). The deviation from the T_C points toward short-range spin correlations that exist in MST.³⁰ Consistent with the MH data, the magnetization in the ab plane is higher than that in the c plane as expected.^{29,30} For comparison, the temperature dependent magnetization data collected on the pristine crystal are also included (see Fig. 2 and supplementary material Fig. S2).

To gain insights into the origin of enhancement in the magnetization at the fluence of 5×10^{15} , the temperature dependent EPR measurements were performed across T_C . EPR is an ideal tool to identify paramagnetic centers that contain unpaired electron spins, local environments, and possible magnetic secondary phases by studying the temperature dependent EPR spectral parameters such as the g -value and signal width.^{35–41} The EPR spectra collected on all the compounds in the ferrimagnetic phase at 50 K are plotted in Fig. 3, which includes both the experimental (dotted curve) and the computer-generated fits (continuous curve) using the Lorentzian and Dysonian line shapes (supplementary material, Fig. S4). From the fits, we identified two overlapped signals. The EPR spectral parameters such as the signal width and g -value (including those of pristine MST) were extracted from the fits and are plotted as a function of fluence (supplementary material, Fig. S5). Upon closer inspection, a clear variation in the EPR spectral parameters is observed at the fluence of around $5 \times 10^{15} \text{ H}^+/\text{cm}^2$. At that fluence, the linewidth for both the signals shows a minimum due to the strong exchange narrowing effect;⁴² the g -value is maximum due to the local enhanced magnetic corrections.⁴³

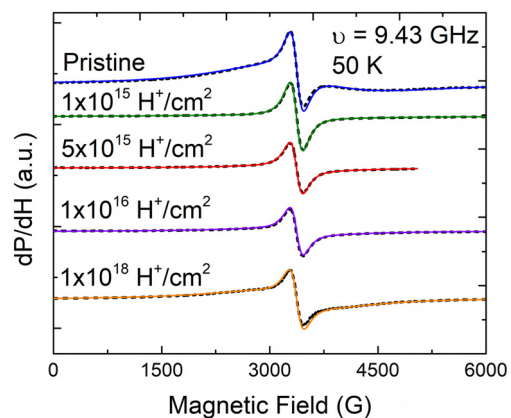


FIG. 3. X-band (9.43 GHz) first derivative EPR spectra measured in the ferrimagnetic phase at 50 K for pristine and the proton irradiated MST crystals as a function of fluence. Continuous curves are the computer-generated fits to the experimental signal shown in dotted curves.

Now, we will assign the two EPR signals. Previous reports^{29,30} show that this compound has two Mn sites, namely, Mn1 (in the *ab* plane) and Mn2 (in the *c* plane). It is also known that the multiplicity of Mn1 is twice that of Mn2 and is significantly separated through distance. This means that the magnetic moment of Mn1 is expected to be two times higher than that of Mn2. The first Mn site (Mn1 site) is composed of MnTe₆ octahedra that are edge-sharing within the *ab*-plane. The Mn2 site links the layers together by filling one-third of the octahedral holes within the vdW gap.³⁰ Due to strong exchange interaction (Mn1–Mn1 ≈ 4.06 Å) among the spins on the Mn1 site, the EPR signal width is expected to be smaller. Hence, it is reasonable to assign the sharper signal ($\Delta H_{pp} \approx 180$ G to 200 G) to Mn1. On the other hand, the broader signal ($\Delta H_{pp} \approx 1200$ G to 1800 G) can be assigned to the Mn2 site. The different surroundings of these two Mn sites produce EPR signals associated with distinct spectral properties. The main signal is sharper, intense, and associated with the *g*-value of 1.998. The broader signal is less intense, associated with *g* ≈ 1.85. The two EPR signals were also observed in the paramagnetic phase (80 K) (supplementary material, Fig. S6). Besides the Mn²⁺ signals (*S* = 5/2; *L* = 0), no additional signals related to (magnetic) defects were observed after proton irradiation. This indicates that the observed changes in magnetization are not due to magnetic defects produced after irradiation. Additionally, hydrogen ion implantation can be ruled out as a likely cause to the change in magnetization because of the lack of hyperfine structures¹² in our EPR spectra of the proton irradiated MST crystals. Fluence dependent magnetic properties were also reflected from the magnetocaloric effect measurements (supplementary material, Fig. S7).

To study the effect of proton irradiation on the lattice vibrations, we performed Raman spectroscopy measurements before and after the irradiation as shown in Fig. 4(a). The peak position as a function of proton fluence, extracted from the fits, is plotted in Fig. 4(b). The Raman spectra for MST have not been previously reported in the literature. However, the Raman spectra for its analog compound CST are reported^{44,45} with peaks arising from the in-plane and out-of-plane Te vibrational modes, which are sensitive to magnetic interactions. The modes seen in the MST Raman spectra located at 118.4 cm⁻¹ with a shoulder at 136.9 cm⁻¹ are close to the peaks found for CST for the E_g³ and A_g³ modes,^{44,45} respectively. The main difference in the spectra of MST and CST arises from the change in the mass and lattice parameter effects that cause the phonon positions to be slightly different.

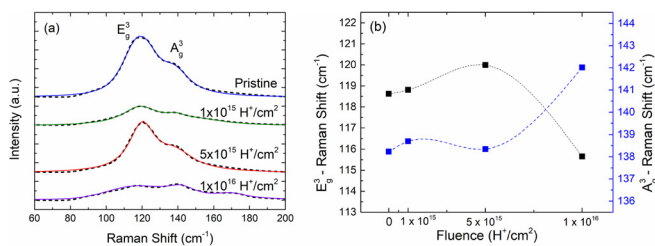


FIG. 4. Raman spectra collected from pristine and proton irradiated MST as a function of fluence; dotted curves are experimental, and the continuous curves are the fits employing the Voigt line shape (a); the peaks shift (including the Raman peak positions for the pristine MST crystal) derived from the fits as a function of proton fluence (b). The room temperature Raman data for 1×10^{18} H⁺/cm² are not available at this point.

From Fig. 4(b), it is found that the change in the E_g³ peak as a function of fluence mimics the observed trend in the M_S shown in Fig. 1(c). Thus, it is very likely that the E_g³ and A_g³ modes involve atomic motions of the Te atoms whose bond strength can be very susceptible to the spin interactions since the Te atoms mediate the super-exchange between the two Cr atoms. While our initial temperature dependent Raman data (supplementary material, Fig. S8) show changes in spectral parameters, indicative of the modification in spin-lattice coupling upon proton irradiation, other factors such as changes in the local band structure and the surface crystal structure could also be at play.

It is more likely that the proton irradiation produced changes in the magnetic interactions within MST. As mentioned before, MST has been shown to contain competing antiferromagnetic interactions that create frustration within the system.³⁰ In particular, the Mn1–Mn1 interactions were reported to have a rivalry between direct interaction (AFM) and Mn1–Te–Mn1 interactions that can lead to FM or AFM, which is determined by whether or not the *p* or *d* orbitals are participating.³⁰ A recent archived report by Ron *et al.* studied the ligand-to-metal charge transfer (CT) in CrSiTe₃.⁴⁶ This was achieved by targeting specific CT transitions in CST using ultrafast laser pulses. They find that by targeting these CT transitions, an enhancement in the nearest-neighbor super-exchange interactions occurs, weakening the AFM direct exchange and thus resulting in an increase in FM exchange. Upon proton irradiation, it is most likely that competing magnetic interactions could be affected by varying the fluence of protons and caused the change in magnetization.

To conclude, we report that the magnetization is significantly enhanced by 53 % and 37 % in the ferrimagnetic phase when the MST was irradiated with the proton fluence of 5×10^{15} , in the *ab* and *c* planes, respectively. From the results obtained from fluence dependent magnetic, EPR, and Raman spectroscopy measurements, we show that the magnetic exchange interactions (Mn–Te–Mn) are modified at this fluence. This work signifies that proton irradiation is very effective in tuning the magnetism of vdW crystals.

See the supplementary material for the proton irradiation depth profile and temperature dependent magnetization measurements performed in both crystallographic directions (*H*//*ab* and *H*//*c*). The χ^{-1} vs temperature curves are presented with their respective CW fits. EPR analysis of the individual signal spectra, at 50 K, for each irradiated crystal along with the pristine crystal is presented. Additionally, the EPR spectra measured at 80 K are also shown with the change in the *g*-value and linewidth, of both signals, as a function of proton fluence. The change in the magnetic entropy is also presented as a function of proton fluence. Finally, low temperature Raman measurements of the pristine and an irradiated crystal (1×10^{18} H⁺/cm²) are presented along with an analysis of the Raman spectra.

L.M.M. acknowledges the useful discussions with H. S. Nair. L.M.M. and S.R.S. acknowledge support from a UTEP start-up grant. L.M.M. acknowledges the Wiemer Family for awarding Student Endowment for Excellence and the NSF-LSAMP B. D. Fellowship. This publication was prepared by S. R. Singamaneni and co-authors under Award No. 31310018M0019 from The University of Texas at El Paso (UTEP), Nuclear Regulatory Commission. The statements, findings, conclusions, and recommendations are those of the author(s) and do not necessarily

reflect the view of the (UTEP) or The U.S. Nuclear Regulatory Commission. The work at Brookhaven National Laboratory was supported by the Office of Basic Energy Sciences, Materials Sciences and Engineering Division, U.S. Department of Energy (DOE) under Contract No. DE-SC0012704. The authors thank S. R. J. Hennadige for his help in EPR measurements. T.T.M. and A.R.H.W. acknowledge the National Institute of Standards and Technology (NIST)/National Research Council Postdoctoral Research Associateship Program and NIST-STRS (Scientific and Technical Research and Services) for funding. Certain commercial equipment, instruments, or materials are identified in this paper in order to specify the experimental procedure adequately. Such identification is not intended to imply recommendation or endorsement by the National Institute of Standards and Technology nor it is intended to imply that the materials or equipment identified are necessarily the best available for the purpose.

REFERENCES

- ¹B. Wang, S. Yang, J. Chen, C. Mann, A. Bushmaker, and S. B. Cronin, *Appl. Phys. Lett.* **111**, 131101 (2017).
- ²A. Geremew, F. Kargar, E. X. Zhang, S. E. Zhao, E. Aytan, M. A. Bloodgood, T. T. Salguero, S. Rummyantsev, A. Fedoseyev, D. M. Fleetwood, and A. A. Balandin, [arXiv:1901.00551](https://arxiv.org/abs/1901.00551) (2019).
- ³R. C. Walker, T. Shi, B. Jariwala, I. Jovanovic, and J. A. Robinson, *Appl. Phys. Lett.* **111**, 143104 (2017).
- ⁴H. Daubric, R. Berger, J. Kliava, G. Chastanet, O. Nguyen, and J.-F. Létard, *Phys. Rev. B* **66**, 054423 (2002).
- ⁵M. Shirai, N. Yonemura, T. Tayagaki, K. Kan'no, and K. Tanaka, *J. Lumin.* **94-95**, 529 (2001).
- ⁶T. Nakayama, O. Yanagisawa, M. Arai, and M. Izumi, *Physica B* **329-333**, 747 (2003).
- ⁷S. Sasaki, Y. F. Zhang, O. Yanagisawa, and M. Izumi, *J. Magn. Magn. Mater.* **310**, 1008 (2007).
- ⁸G. Yang, S. Jang, F. Ren, S. J. Pearton, and J. Kim, *ACS Appl. Mater. Interfaces* **9**, 40471 (2017).
- ⁹C. Claeys and E. Simoen, *Radiation Effects in Advanced Semiconductor Materials and Devices* (Springer-Verlag, Berlin Heidelberg, 2002).
- ¹⁰A. V. Krasheninnikov and K. Nordlund, *J. Appl. Phys.* **107**, 071301 (2010).
- ¹¹P. Esquinazi, D. Spemann, R. Höhne, A. Setzer, K.-H. Han, and T. Butz, *Phys. Rev. Lett.* **91**, 227201 (2003).
- ¹²K. W. Lee and C. E. Lee, *Phys. Rev. Lett.* **97**, 137206 (2006).
- ¹³S. W. Han, Y. H. Hwang, S.-H. Kim, W. S. Yun, J. D. Lee, M. G. Park, S. Ryu, J. S. Park, D.-H. Yoo, S.-P. Yoon, S. C. Hong, K. S. Kim, and Y. S. Park, *Phys. Rev. Lett.* **110**, 247201 (2013).
- ¹⁴T. L. Makarova, A. L. Shelankov, I. T. Serenkov, V. I. Sakharov, and D. W. Boukhvalov, *Phys. Rev. B* **83**, 085417 (2011).
- ¹⁵M. A. Ramos, J. Barzola-Quiquia, P. Esquinazi, A. Muñoz-Martin, A. Climent-Font, and M. García-Hernández, *Phys. Rev. B* **81**, 214404 (2010).
- ¹⁶S. Mathew, K. Gopinadhan, T. K. Chan, X. J. Yu, D. Zhan, L. Cao, A. Rusydi, M. B. H. Breese, S. Dhar, Z. X. Shen, T. Venkatesan, and J. T. L. Thong, *Appl. Phys. Lett.* **101**, 102103 (2012).
- ¹⁷H. Ohldag, P. Esquinazi, E. Arenholz, D. Spemann, M. Rothermel, A. Setzer, and T. Butz, *New J. Phys.* **12**, 123012 (2010).
- ¹⁸R.-W. Zhou, X.-C. Liu, H.-J. Wang, W.-B. Chen, F. Li, S.-Y. Zhuo, and E.-W. Shi, *AIP Adv.* **5**, 047146 (2015).
- ¹⁹P. Esquinazi, R. Höhne, K.-H. Han, A. Setzer, D. Spemann, and T. Butz, *Carbon* **42**, 1213 (2004).
- ²⁰T.-Y. Kim, K. Cho, W. Park, J. Park, Y. Song, S. Hong, W.-K. Hong, and T. Lee, *ACS Nano* **8**, 2774 (2014).
- ²¹Y. Yu, S.-Y. Huang, Y. Li, S. N. Steinmann, W. Yang, and L. Cao, *Nano Lett.* **14**, 553 (2014).
- ²²S. Yan, W. Qiao, X. He, X. Guo, L. Xi, W. Zhong, and Y. Du, *Appl. Phys. Lett.* **106**, 012408 (2015).
- ²³X. Ren, L. Pang, Y. Zhang, X. Ren, H. Fan, and S. (Frank) Liu, *J. Mater. Chem. A* **3**, 10693 (2015).
- ²⁴L. M. Martinez, J. A. Delgado, C. L. Saiz, A. Cosio, Y. Wu, D. Villagrán, K. Gandha, C. Karthik, I. C. Nlebedim, and S. R. Singamaneni, *J. Appl. Phys.* **124**, 153903 (2018).
- ²⁵P. Ajayan, P. Kim, and K. Banerjee, *Phys. Today* **69**(9), 38 (2016).
- ²⁶K. S. Burch, D. Mandrus, and J.-G. Park, *Nature* **563**, 47 (2018).
- ²⁷D. L. Duong, S. J. Yun, and Y. H. Lee, *ACS Nano* **11**, 11803 (2017).
- ²⁸A. F. May, D. Ovchinnikov, Q. Zheng, R. Hermann, S. Calder, B. Huang, Z. Fei, Y. Liu, X. Xu, and M. A. McGuire, *ACS Nano* **13**, 4436 (2019).
- ²⁹Y. Liu and C. Petrovic, *Phys. Rev. B* **98**, 064423 (2018).
- ³⁰A. F. May, Y. Liu, S. Calder, D. S. Parker, T. Pandey, E. Cakmak, H. Cao, J. Yan, and M. A. McGuire, *Phys. Rev. B* **95**, 174440 (2017).
- ³¹R. C. Walker, T. Shi, E. C. Silva, I. Jovanovic, and J. A. Robinson, *Phys. Status Solidi A* **213**, 3065 (2016).
- ³²A. Geremew, F. Kargar, E. X. Zhang, S. E. Zhao, E. Aytan, M. A. Bloodgood, T. T. Salguero, S. Rummyantsev, A. Fedoseyev, D. M. Fleetwood, and A. A. Balandin, [arXiv:1901.00551](https://arxiv.org/abs/1901.00551) (2019).
- ³³L. Shao, J. Gigax, D. Chen, H. Kim, F. A. Garner, J. Wang, and M. B. Toloczko, *Nucl. Instrum. Methods Phys. Res., Sect. B* **409**, 251 (2017).
- ³⁴J. G. Gigax, H. Kim, E. Aydogan, F. A. Garner, S. Maloy, and L. Shao, *Mater. Res. Lett.* **5**, 478 (2017).
- ³⁵C. L. Saiz, M. A. McGuire, S. R. J. Hennadige, J. van Tol, and S. R. Singamaneni, *MRS Adv.* **4**, 2169 (2019).
- ³⁶G. R. HariPriya, C. M. N. Kumar, R. Pradheesh, L. M. Martinez, C. L. Saiz, S. R. Singamaneni, T. Chatterji, V. Sankaranarayanan, K. Sethupathi, B. Kiefer, and H. S. Nair, *Phys. Rev. B* **99**, 184411 (2019).
- ³⁷L. M. Martinez, C. Karthik, M. Kongara, and S. R. Singamaneni, *J. Mater. Res.* **33**, 1565 (2018).
- ³⁸S. R. Singamaneni, J. van Tol, R. Ye, and J. M. Tour, *Appl. Phys. Lett.* **107**, 212402 (2015).
- ³⁹H. S. Nair, R. Yadav, S. Adiga, S. S. Rao, J. van Tol, and S. Elizabeth, *Physica B* **456**, 108 (2015).
- ⁴⁰S. S. Rao, A. Stesmans, J. van Tol, D. V. Kosynkin, A. Higginbotham-Duque, W. Lu, A. Sinitkii, and J. M. Tour, *ACS Nano* **6**, 7615 (2012).
- ⁴¹S. S. Rao, A. Stesmans, D. V. Kosynkin, A. Higginbotham, and J. M. Tour, *New J. Phys.* **13**, 113004 (2011).
- ⁴²P. M. Richards and M. B. Salamon, *Phys. Rev. B* **9**, 32 (1974).
- ⁴³N. S. Sangeetha, S. D. Cady, and D. C. Johnston, [arXiv:1809.02653](https://arxiv.org/abs/1809.02653) (2018).
- ⁴⁴A. Milosavljević, A. Šolajić, J. Pešić, Y. Liu, C. Petrovic, N. Lazarević, and Z. V. Popović, *Phys. Rev. B* **98**, 104306 (2018).
- ⁴⁵M.-W. Lin, H. L. Zhuang, J. Yan, T. Z. Ward, A. A. Puretzy, C. M. Rouleau, Z. Gai, L. Liang, V. Meunier, B. G. Sumpter, P. Ganesh, P. R. C. Kent, D. B. Geohegan, D. G. Mandrus, and K. Xiao, *J. Mater. Chem. C* **4**, 315 (2016).
- ⁴⁶A. Ron, S. Chaudhary, G. Zhang, H. Ning, E. Zoghlin, S. D. Wilson, R. D. Averitt, G. Refael, and D. Hsieh, [arXiv:1910.06376](https://arxiv.org/abs/1910.06376) (2019).